Dust formation in oxygen–rich environments under oscillating thermodynamic conditions

KYUNG SOOK JEONG, JAN MARTIN WINTERS,
AXEL J. FLEISCHER, ERWIN SEDLMAYR

Institut f. Astronomie & Astrophysik, TU Berlin, Germany

Poster contribution presented at *A half century of stellar pulsation interpretations: A tribute to Arthur N. Cox* , June 16–20 1997, Los Alamos, New Mexico

1 Introduction

Circumstellar shells around cool, pulsating late type stars are well known sites of copious dust formation. According to the abundance ratio between oxygen and carbon, these objects are classified into three major groups: M stars ($\epsilon_{\rm C} < \epsilon_{\rm O}$), S stars ($\epsilon_{\rm C} \approx \epsilon_{\rm O}$),and C stars ($\epsilon_{\rm C} > \epsilon_{\rm O}$), where the M stars constitute by far the largest group.

Since these objects are loosing mass at high rates, they serve as the major source for replenishing the interstellar medium with processed material, in particular in the form of complex molecules and of solid dust particles.

In contrast to the carbon–rich situation, where mainly *homogeneous* amorphous carbon grains are formed in an oxygen–rich environment almost all carbon is locked up in the chemically inert CO molecule. Therefore, the grains only can be formed from molecules containing the remaining oxygen and the less abundant elements Mg, Si, S, Fe, Al and Ti. In this case a *heterogeneous* element composition of the emerging dust component has to be expected.

To focus the investigation on the heterogeneous condensation of these elements, in this poster we consider a gas element which is subject to periodic variations of temperature and density in order to simulate the varying conditions encountered by gas elements moving through the circumstellar shell of an oxygen–rich LPV.

2 Modeling method

Assuming chemical equilibrium in the gas phase, we describe the nucleation process of the seed particles by means of classical nucleation theory according to the equations given in Gail et al. (1984).These seed nuclei (homogeneous SiO, Fe, TiO and TiO_2 clusters, cf. Gail & Sedlmayr (1986)) grow by addition of those molecular species which have a stable solid phase under the local thermodynamic conditions prevailing in the circumstellar environment.

Heterogeneous growth of the particles is treated by means of a moment method (Dominik et al. 1993), while grain evaporation is described by the formalism developed in Gauger et al. (1990).

- We consider an **adiabatic gas element** with a prescribed sinusoidal temporal variation of the temperature. Correspondingly, also the density varies sinusoidally in time. The values of the period P, the mean temperature $\bar{T}$, the temperature amplitude ΔT, and the mean density $\bar{\rho}$ as well as the value of the adiabatic exponent γ are given in Tab. 1.

- Under these thermal scenarios, nucleation of seed particles, heterogeneous growth, and thermal evaporation of dust grains is investigated in an oxygen–rich environment.

- The nucleation rates of potential nuclei

◇ Fig. 1 shows the nucleation rates in a gas element. Seed nuclei become stable at different temperatures: Al_2O_3 at 1360 K, TiO_2 at 1160 K, TiO at 1140 K, Fe at 920 K, SiO at 730 K.

◇ In the P-T plane we can see the more distinct differences in the nucleation rates of diverse seeds (cf. Fig. 2).

Al_2O_3 has its maximum nucleation rate at high temperature (1100 K), but the nucleation rate is so small that it is negligible, as is same for TiO.

We choose Fe and TiO_2 for nucleation seeds, because the nucleation of SiO does not occur till the lower temperature, although SiO has the most effective nucleation rate.

- Nucleation of homogeneous Fe– and TiO_2–clusters as seed nuclei is considered.

Table 1: Parameters for the calculation

P	$\bar{T}$	ΔT	$\bar{\rho}$	γ
[d]	[K]	[K]	[g cm^{-3}]	
300	1100	700	10^{-13}	5/3

3 Results

Heterogeneous growth on Fe nuclei

- Nucleation of Fe starts around T = 920 K, with a maximum nucleation rate around T = 690 K; see Fig. 3.

- The different species successively contribute to grain growth (cf. Fig. 4), according to a stability hierarchy established by the thermodynamic properties of growing molecules. The last element contributing to growth is **sulphur**.

- Growth of particles up to an average size of $\sim 7 \cdot 10^{-3} \mu$m.

- All dust–forming elements become completely depleted from the gas phase (cf. Fig. 4), with the exception of oxygen, because most of oxygen is in H_2O.

- Evaporation of S occurs around T = 680 K, of Fe around T = 1200 K, and of Si around T = 1360 K. After evaporation of Fe in the grain mantle, the Fe core is still present up to T = 1600 K, since it is surrounded by the very stable aluminium bearing molecules.

- Complete destruction of grains occurs at T = 1600 K. Destruction of the cores occurs in a very narrow temperature range.

Heterogeneous growth on TiO_2 nuclei

- Nucleation of TiO_2 starts around $T = 1160$ K, with a maximum nucleation rate around $T = 830$ K; see Fig. 5. This lets growth of grains more higher temperature than that on Fe–nuclei.
- The mean particle radius becomes larger, up to $1{\cdot}10^{-2}\mu$m (cf. Fig. 5) and the number of dust particles is less than in the case of Fe nuclei.
- O, Si, S and Ti are not completely depleted.

Acknowledgements: This work has been supported by the FAZIT Stiftung, the DFG (grant Se 420/8–1), the BMBF (grant 05 3BT13A 6).

References

Dominik, C., Sedlmayr, E., and Gail, H.-P., 1993. Dust formation in stellar winds. VI. Moment equations for the formation of heterogeneous and core-mantle grains. *A&A*, **277**, 578–594.
Gail, H.-P. and Sedlmayr, E., 1986. The primary condensation process for dust around late M-type stars. *A&A*, **166**, 225–236.
Gail, H.-P., Keller, R., and Sedlmayr, E., 1984. Dust formation in stellar winds. I. A rapid computational method and application to graphite condensation. *A&A*, **133**, 320–332.
Gauger, A., Gail, H.-P., and Sedlmayr, E., 1990. Dust formation, growth and evaporation in a cool pulsating circumstellar shell. *A&A*, **235**, 345–361.

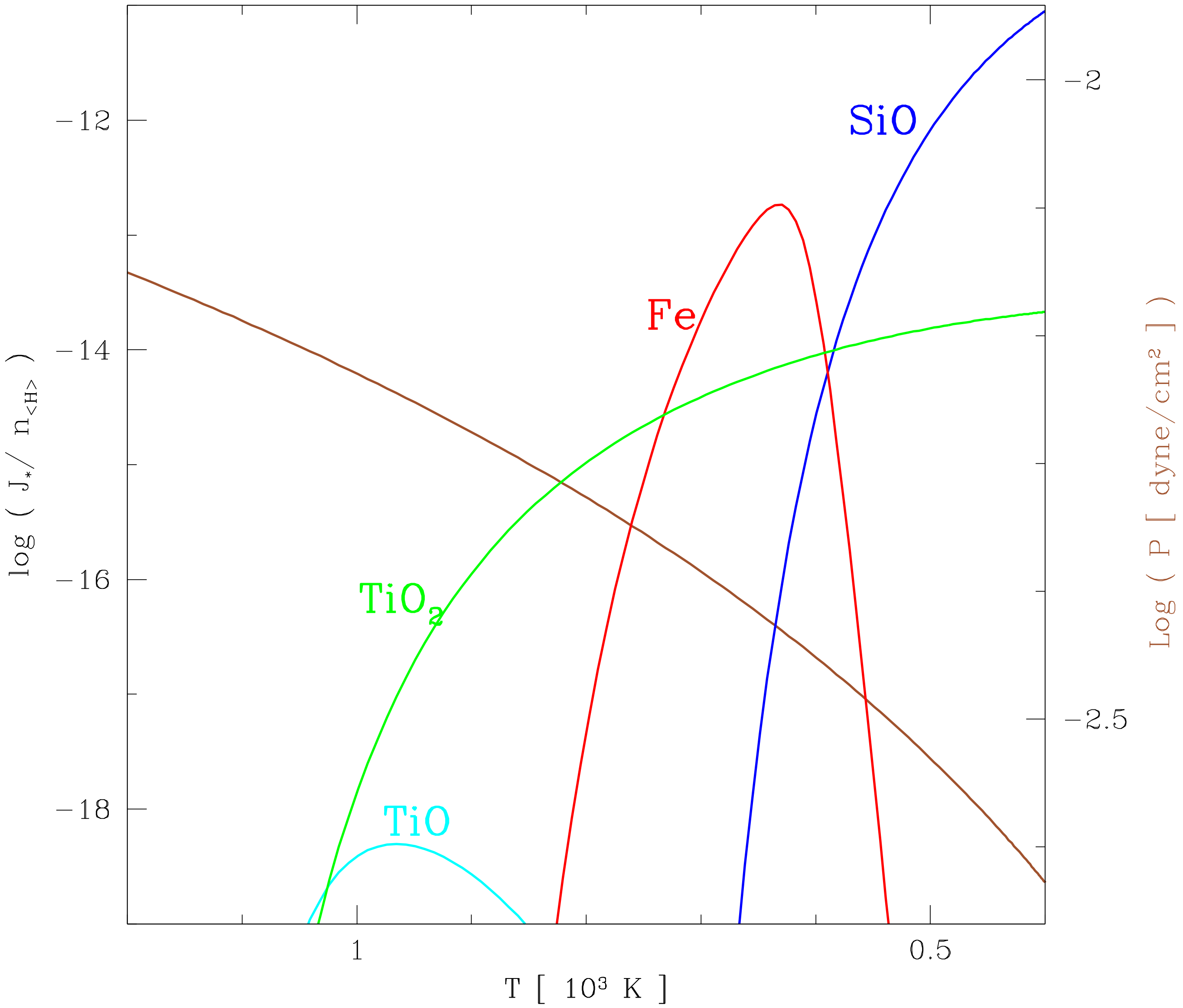

Figure 1: Nucleation rates J_* for different nuclei.

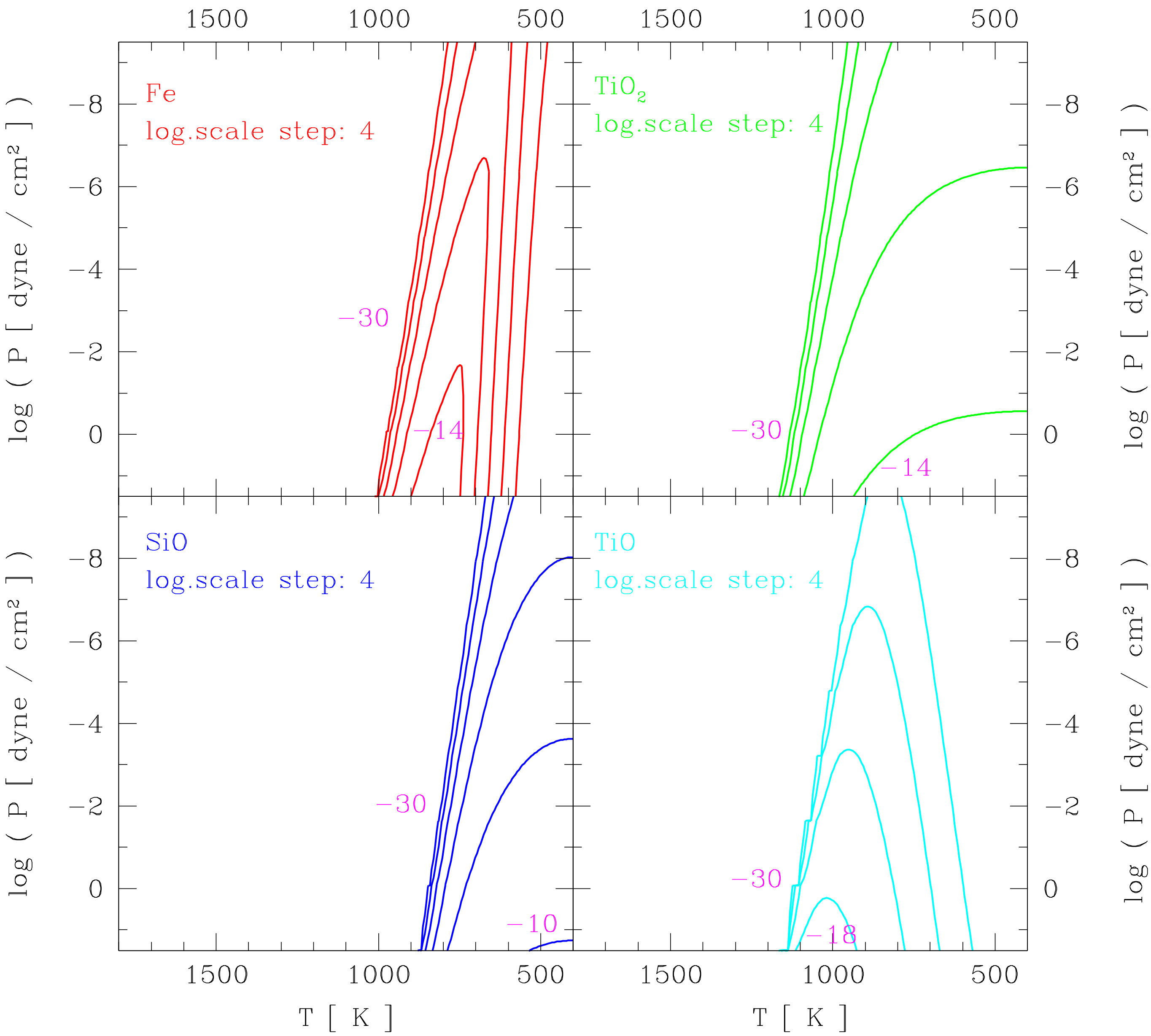

Figure 2: Nucleation rates in the P-T plane.
The contours are the logarithm of the nucleation rates in [-30, -10].
The logarithmic scale step is 4.

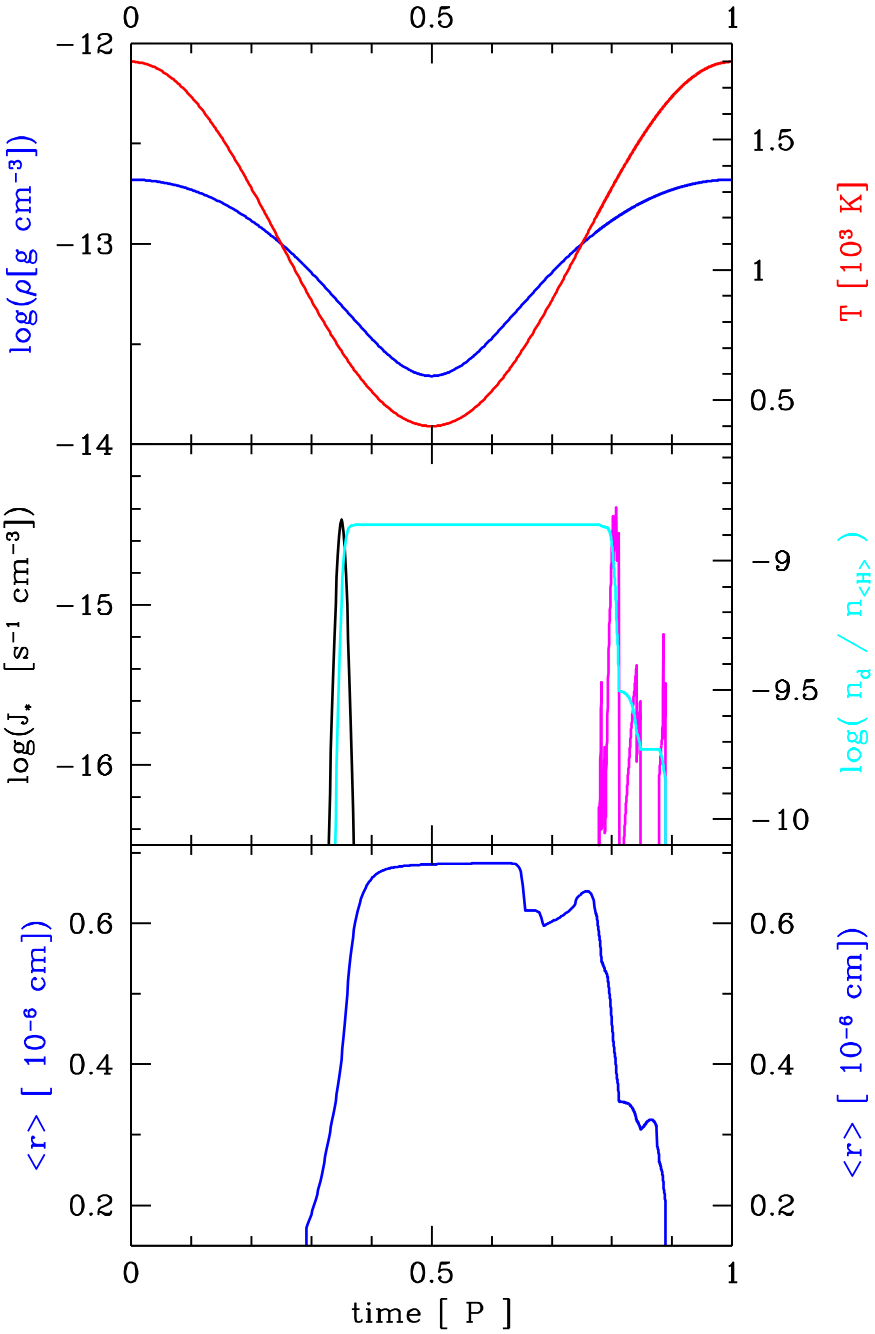

Figure 3: Thermodynamical and dust quantities for Fe nuclei.
upper diagram: logarithm of the mass density ρ (blue line, l.h.s. ordinate) and Temperature T (red line, r.h.s. ordinate); **middle diagram:** logarithm of the nucleation and evaporation rate J_* and $J_{\rm ev}$ ($J_{*,\rm Fe}$: black line, $J_{\rm ev}$ magenta line, l.h.s. ordinate) and logarithm of the number of dust particles per H–atom $n_{\rm d}/n_{<\rm H>}$ (blue line, r.h.s. ordinate); **lower diagram:** mean particle radius $< \rm r >$.

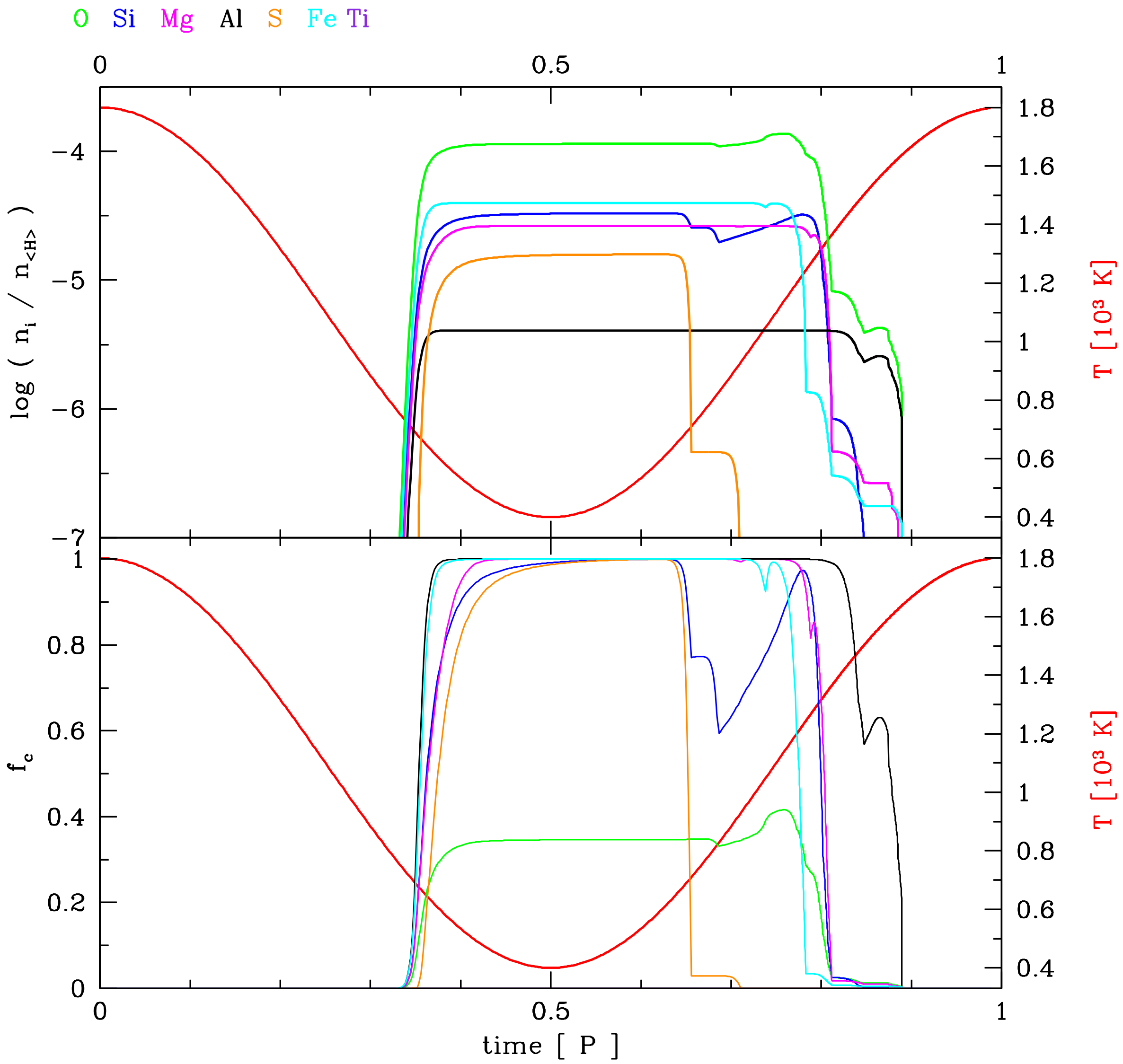

Figure 4: Chemical composition of the dust grains as a function of time for Fe nuclei. **upper diagram:** logarithm of the number of condensed atoms of element i per H–atom $n_i/n_{<\mathrm{H}>}$, **lower diagram:** Degree of condensation f_c of the considered elements.

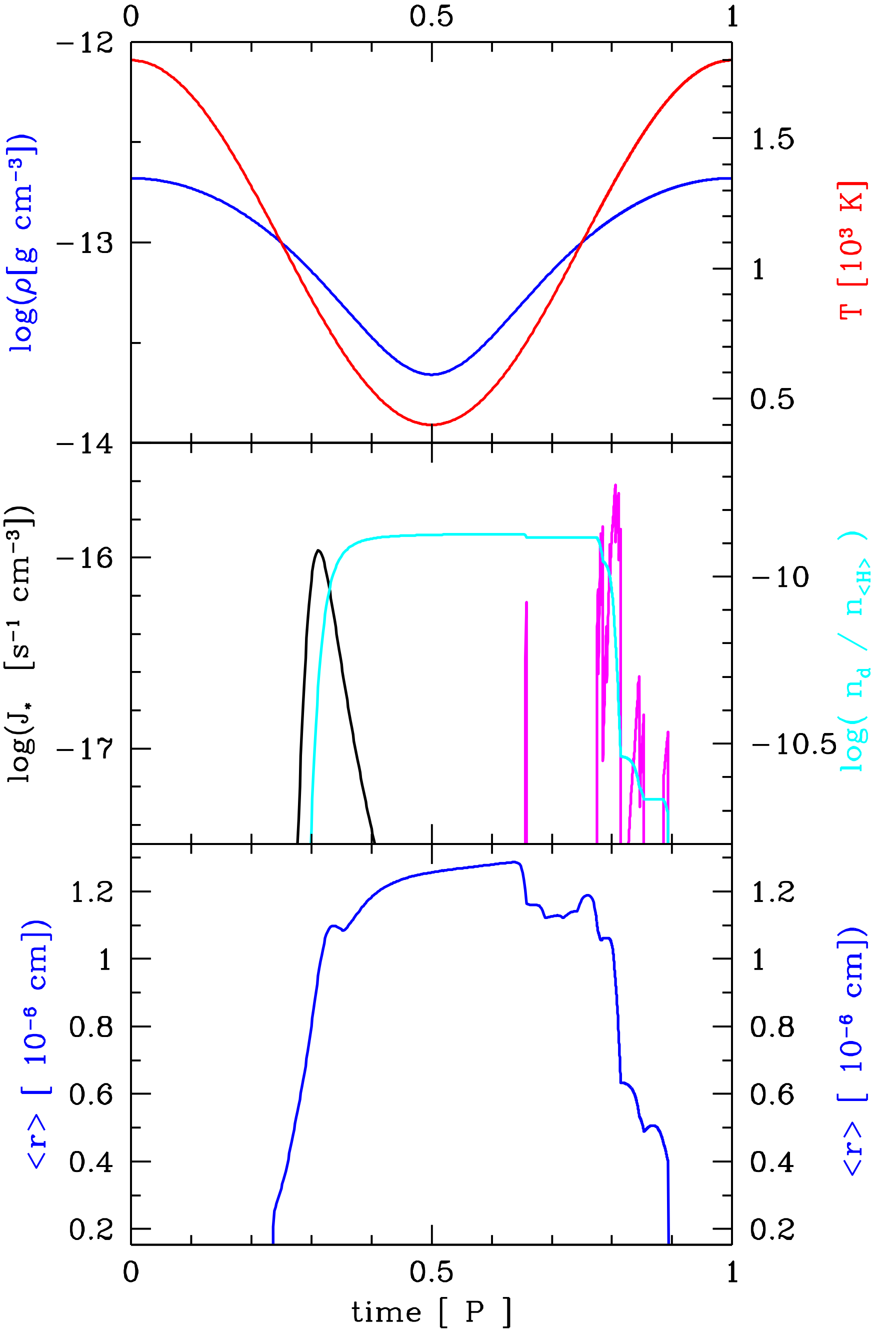

Figure 5: Thermodynamical and dust quantities for TiO_2 nuclei.
upper diagram: logarithm of the mass density ρ (blue line, l.h.s. ordinate) and Temperature T (red line, r.h.s. ordinate); **middle diagram:** logarithm of the nucleation and evaporation rate J_* and $J_{\rm ev}$ ($J_{*,\rm Fe}$: black line, $J_{\rm ev}$ magenta line, l.h.s. ordinate) and logarithm of the number of dust particles per H–atom $n_{\rm d}/n_{<\rm H>}$ (blue line, r.h.s. ordinate); **lower diagram:** mean particle radius $< \mathrm{r} >$.

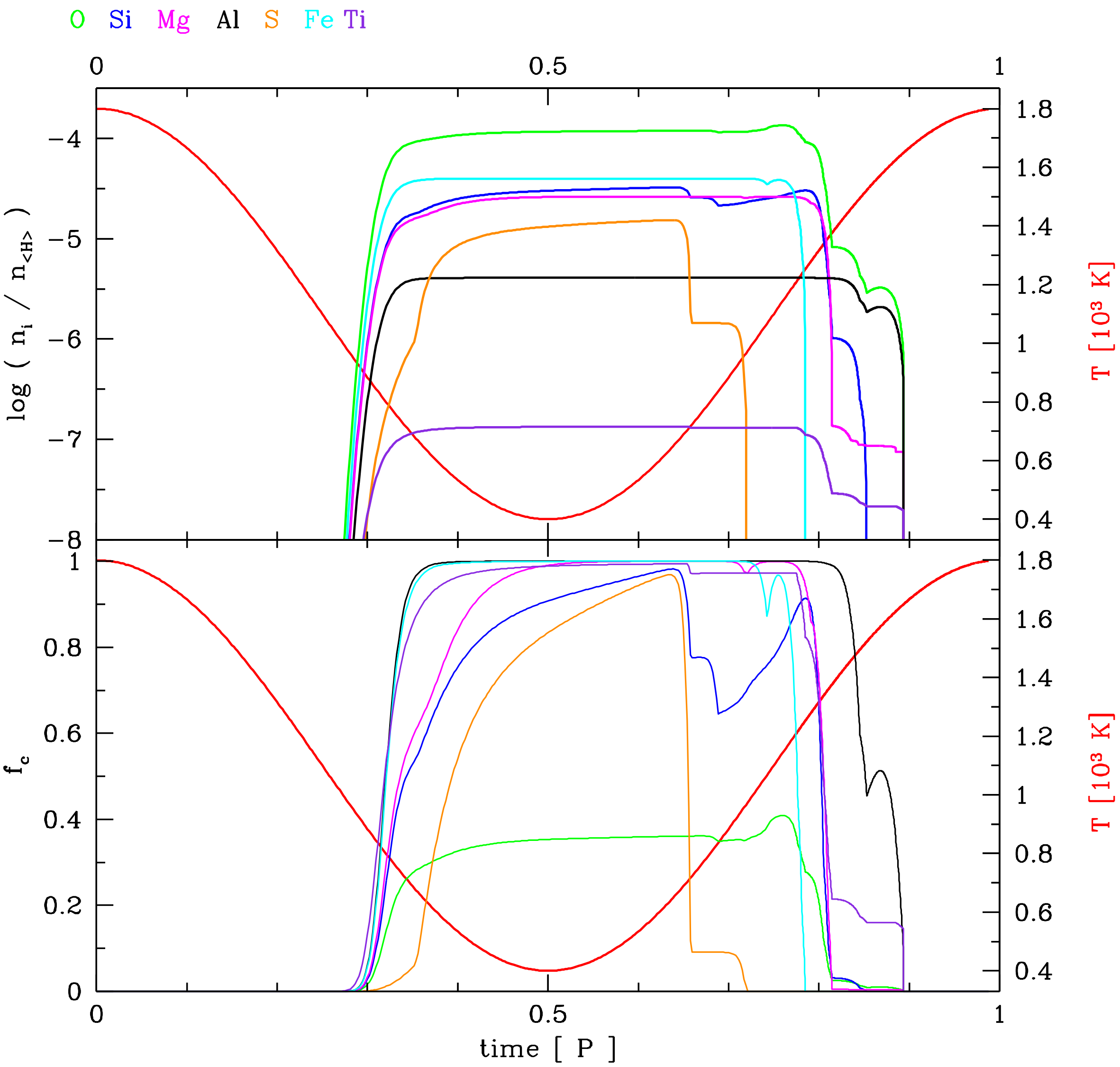

Figure 6: Chemical composition of the dust grains as a function of time for TiO_2 nuclei. **upper diagram:** logarithm of the number of condensed atoms of element i per H–atom $n_i/n_{<\mathrm{H}>}$, **lower diagram:** Degree of condensation f_c of the considered elements.